# New calibration sources for very long baseline interferometry in the 1.4-GHz band

**M K Hailemariam[1,2], M F Bietenholz[2], A de Witt[2], R S Booth[1]**

[1] Department of Physics, University of Pretoria, South Africa

[2] Hartebeesthoek Radio Astronomy Observatory (HartRAO), South Africa

E-mail: mekunet@gmail.com

**Abstract.** We present new 1.6 GHz observations of 43 VLBI calibrator sources. Our goal was mainly to establish the suitability of the sources as calibrators for 1.4-GHz band VLBI observations. We used seven telescopes; ASKAP, ATCA, Ceduna, Hobart, Mopra and Parkes from Australia, and HartRAO from South Africa. We classified the sources into 4 categories according to their suitability as calibrators in the 1.4-GHz band by determining their angular size, total flux density and the fraction of the flux density in the central component. Of the 43 sources, we found that 38 sources fell in to the good or very good calibrator classes. On the basis of selected sources from our sample we found that 91% of the good calibrators at 8.4 GHz are also safe to use as calibrator in the 1.4-GHz band.

## 1. Introduction

Relatively few Very Long Baseline Interferometry (VLBI) calibrator sources are known in the Southern celestial Hemisphere especially in the 1.4-GHz band (1-2 GHz). This is mainly due to the smaller number of observing facilities in the south compared to in the north. There are different surveys underway to increase the number of calibrator sources in the Southern Hemisphere, but most of these surveys are focused on observations at frequencies higher than 2 GHz, for example 8.4 GHz and 2.3 GHz (e.g. [8, 11, 12]), and there are virtually no VLBI calibrator observations at frequencies $< 2$ GHz. The small number of known calibrator sources and antennas in the Southern Hemisphere makes VLBI observation more difficult.

New VLBI-capable telescopes are coming to the south, in particular operating at $< 2$ GHz. ASKAP ($< 2$ GHz only) and MeerKAT ($< 2$ GHz and higher frequencies) are the two telescope arrays currently being built by Australia and South Africa respectively ([2, 9]). The African VLBI Network (AVN) is another big project in Africa, which aims to use redundant large telecommunication antennas across the continent for radio astronomy [7]. Despite the increasing number of antennas in the Southern Hemisphere, the number of calibrator sources in the 1.4-GHz band, for VLBI observations are very few. The high demand for calibrator sources at frequencies $< 2$ GHz, especially in the future, is the major motivation to look for calibrator sources in the 1.4-GHz band.

Most VLBI observations rely on observations of calibrator sources. An ideal calibrator source would look the same on all observing baselines which implies that it has to be unresolved (point-like). A calibrator source should also be bright, so that it can be observed with high signal to noise ratio on all baselines, and have an accurately known position. Almost all calibrator sources used for VLBI observations are Active Galactic Nuclei (AGN) [1, 10]. AGN are the active nuclei within galaxies thought to be due to accretion onto super massive black holes. These extra-galactic radio sources, AGN, are very distant objects and therefore, generally, have no discernible proper motions on the sky.

Our research involved the reduction and analysis of VLBI observations of 43 sources in the Southern Hemisphere, at 1.6 GHz (see section 2). We determined the suitability of these sources as calibrators at 1.6 GHz, and compare the results of our observations to other 8.4 GHz observations to see how safe it is to use known 8.4 GHz calibrator sources for 1.4-GHz band observations.

## 2. Data Selection and Observations

We selected our sample of 43 sources from the Radio Fundamental Catalog (RFC[1]) of compact radio sources [1, 6, 10, 12, 13, 14, 15]. In the catalog, we found 1131 sources with declinations $< -30°$ and that had only been observed at 8.4 GHz. Of these, we found 77 sources with a flux density $> 500$ mJy that are listed as suitable calibrator sources at 8.4 GHz. Among the 77 sources, we selected the 25 sources for which 8.4 GHz images are available and the brightest 9 of the remainder. In order to cover all Right Ascensions for our 24-hour observations we also included 7 sources listed in the RFC as non-calibrator sources. We finally added two additional sources, to use as fringe finders.

We observed the sources at 1.6 GHz, with total band width of 8 MHz, using seven antennas: ASKAP (single 12-m dish), ATCA, Ceduna, Hobart, Mopra and Parkes from Australia, and HartRAO from South Africa. The observations were carried out between 22 and 23 February 2015. We used the Astronomical Image Processing System (AIPS[2]) software to calibrate the data.

## 3. Results and Discussion

After the final calibration we did the imaging (i.e. inverse Fourier transform of calibrated visibility data) using the same software (AIPS) that we used for the data reduction. The resulting inverse Fourier transform of the sampled visibility is the convolution of the true brightness distribution and the dirty beam [3, 5]. To recover the true intensity distribution we used a deconvolution algorithm called CLEAN [4]. CLEAN is an iterative process which represents an estimate of the true sky brightness as a series of delta functions, called CLEAN components.

In Table 1, we list the total flux density ($S_{\rm CL}$) for each of the sources we imaged, which is the sum of the flux densities of the CLEAN components in the image. We also list the peak brightness ($B_{\rm P}$) and off-source rms brightness ($B_{\rm orms}$), which we use as an estimate of the brightness noise level of the images, for each of the sources we imaged. The average radius of the beams from our observations is 2.6 milliarcsecond (mas). The values of the $B_{\rm p}$ range from 118 mJy beam$^{-1}$ to 2720 mJy beam$^{-1}$ and $B_{\rm orms}$ ranges from 2.2 mJy beam$^{-1}$ to 20.4 mJy beam$^{-1}$. The mean value of the image dynamic range ($B_{\rm p}/B_{\rm orms}$) was 60, which is sufficient to determine whether or not the sources will make good calibrators. Images of some of the sources are shown in Figure 1

### 3.1. Core fraction

Next we calculated the core fraction and the radial extents of our sources to evaluate if they are compact enough to be used as calibrators. The core fraction, **C**, of a source is the ratio of the flux density in the unresolved core to the total flux density [11]. We define the core flux density as the sum of the CLEANed flux density within an angular radius of 2.5 mas from the brightest

[1] Available on the Web at http://astrogeo.org/rfc/
[2] http://www.aips.nrao.edu

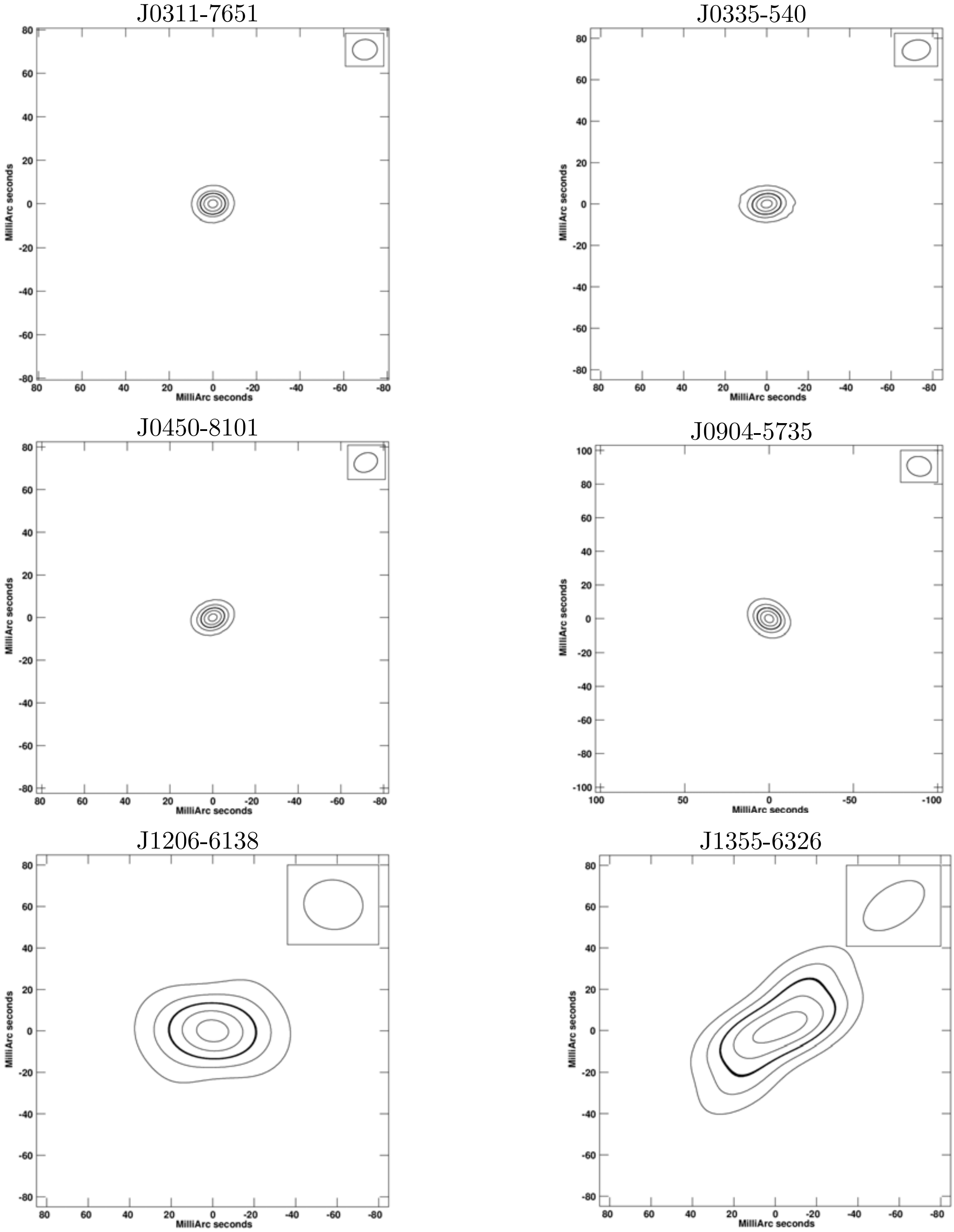


**Figure 1.** Contour plots of the brightness distribution as an example of compact (J0311-7651, J0335-540, J0450-8101, J0904-5735) and extended (J1206-6138, J1355-6326) sources in our sample. The contours are drawn at 10, 30, 50,70 and 90 percent of the peak brightness with the 50 percent contour being darker than the rest. The FWHM of the convolving beam is shown in the upper right in each panel.

**Table 1.** Image Parameters: the peak brightness ($B_{\rm P}$), the image off-source rms brightness ($B_{orms}$) and the total CLEAN flux densities ($S_{CL}$)

| Source (J2000 name) | $B_{\rm P}$ (Jy/beam) | $B_{orms}$ (mJy/beam) | $S_{\rm CL}$ (mJy) | Source | $B_{\rm P}$ (Jy/beam) | $B_{orms}$ (mJy/beam) | $S_{\rm CL}$ (mJy) |
|---|---|---|---|---|---|---|---|
| J0058-5659 | 361 | 6.3 | 369 | J1424-6807 | 712 | 13.2 | 752 |
| J0253-5441 | 678 | 16.1 | 687 | J1427-4206 | 2000 | 2.3 | 2252 |
| J0311-7651 | 486 | 9.6 | 498 | J1512-5640 | 238 | 7.9 | 418 |
| J0335-5430 | 260 | 5.5 | 281 | J1515-5559 | 830 | 18.3 | 1020 |
| J0450-8101 | 686 | 11.2 | 706 | J1624-6809 | 1030 | 17.8 | 1060 |
| J0529-7245 | 423 | 14.1 | 429 | J1628-6152 | 367 | 5.2 | 400 |
| J0743-6726 | 841 | 20.4 | 898 | J1703-6212 | 467 | 5.2 | 566 |
| J0904-5735 | 251 | 3.7 | 252 | J1744-5144 | 2720 | 4.9 | 3650 |
| J1038-5311 | 440 | 7.5 | 496 | J1803-6507 | 469 | 6.2 | 489 |
| J1041-4740 | 891 | 13.2 | 974 | J1809-4552 | 226 | 4.1 | 263 |
| J1051-5344 | 841 | 15.4 | 905 | J1837-7108 | 723 | 13.9 | 755 |
| J1101-6325 | 566 | 9.4 | 735 | J1912-8010 | 536 | 16.2 | 550 |
| J1107-6820 | 502 | 10.0 | 521 | J1930-6056 | 527 | 9.9 | 660 |
| J1112-5703 | 381 | 2.5 | 539 | J1940-6907 | 795 | 13.4 | 830 |
| J1131-5818 | 469 | 4.5 | 491 | J2035-6846 | 118 | 2.4 | 121 |
| J1145-6954 | 274 | 4.4 | 279 | J2105-7825 | 260 | 5.2 | 265 |
| J1151-6728 | 914 | 18.0 | 1080 | J2147-7536 | 755 | 12.1 | 768 |
| J1206-6138 | 134 | 2.2 | 232 | J2152-7807 | 496 | 5.3 | 509 |
| J1252-6737 | 430 | 4.3 | 298 | J2303-6807 | 456 | 7.4 | 468 |
| J1254-7138 | 470 | 10.5 | 487 | J2336-5236 | 1190 | 19.8 | 1250 |
| J1315-5334 | 178 | 3.0 | 218 | J2356-6820 | 482 | 9.4 | 522 |
| J1355-6326 | 285 | 17.6 | 728 | | | | |

point in the image. An angular radius of 2.5 mas is representative of the resolution obtained in global baselines (and also of the maximum resolution we obtained in our observations). Only 7 of our sources have $\mathbf{C} < 0.75$. This shows that most of our sources are largely dominated by the core or most of the flux densitiy is concentrated in the central component. The values of **C** are listed in Table 2.

### 3.2. Radial extent

We calculated three types of radial extent measurements. The first one is the flux-weighted radial extent of the sources, which is given by

$$r_{\rm wt} = \frac{\sum_i S_{\rm i} r_{\rm i}}{\sum_i S_{\rm i}} \tag{1}$$

Where $r_{\rm i}$ is the radius from the brightest point of the $i^{th}$ CLEAN component, and $S_{\rm i}$ its flux density. The flux weighted radial extent of the sources ranges from 0.41 to 5.36 mas, with a mean of 1.57 mas.

The second type of radial extent measurement is the 95 percent flux-density radius, $r_{95\%}$, which is the radius within which 95 percent of the flux density of the source is contained, also measured from the brightest point in the image. We determined $r_{95\%}$ by adding the flux densities of the CLEAN components in order of increasing radius until we get 95 percent of the $S_{\rm CL}$. The $r_{95\%}$ ranges from 0.82 to 16.89 mas, with the mean equal to 4.13 mas.

Our third type of radial extent measurement, which is the half-width-at-half-maximum (HWHM) radius of a circular Gaussian whose Fourier transform was fitted directly to the visibilities by least squares (thus by passing the CLEAN deconvolution). The HWHM of the sources ranges from 0.3 mas to 12.8 mas, with the mean equal to 2.19 mas.

Finally, we take the mean of $r_{\rm wt}$, $r_{95\%}$ and the HWHM for each source to get an average radius of $r_{\rm av}$. We list the values of the $r_{\rm av}$ in Table 2.

## 4. Classification of Calibrator Quality

We determined whether our sources were suitable for use as calibrators by using $r_{av}$ described in the previous section. We divided the sources into four groups, according to their calibrator quality, as follows:

- **Very Good (VG)**:- contains sources with core fraction C $\geq$ 0.8 and average radius $r_{av} \leq$ 0.4 mas. We have 31 sources in this group all of which have sufficient flux density on all baselines.
- **Good (G)**: contains sources which are not in the first group but which have C $\geq$ 0.5 and $r_{av} \leq$ 6 mas. They also have sufficient flux density on all baselines. We found seven of our sources in this group.
- **Intermediate (I)**: contains sources which are not in the first or the second group but which have C $\geq$ 0.5 and $r_{av} <$ 8 mas or C $>$ 0.3 and $r_{av} <$ 0.6 mas. We only have one source in this group. This source doesn't have sufficient flux density on HartRAO baselines.
- **Bad (B)**: contains sources which are not in the other three groups.

In addition to compactness and brightness, calibrator sources should have accurately known positions. Among our 43 sources, the 35 sources which are listed as calibrators[3] (see Table 2) in the RFC, have accurately determined positions and are good calibrators at 8.4 GHz. Out of the 35 sources with accurate positions, 32 (91%) sources fell in to the good or very good calibrator classes. The remaining 8 sources, which are listed as non-calibrators[4], have source positions with large uncertainties. It is important to classify not only the 35 sources but also the 8 sources, because we could get better positions for those 8 sources in future.

**Table 2.** The average radius, $r_{av}$, the core fraction, **C**, calibrator class of the sources (VG for Very Good, G for Good, I for Intermediate and B for Bad) and status of the sources in the rfc_2016b catalog (C– Calibrator and N– Non-calibrator)

| Source | $r_{av}$ | **C** | Class | RFC Status | Source | $r_{av}$ | **C** | Class | RFC Status |
|---|---|---|---|---|---|---|---|---|---|
| J0058-5659 | 0.74 | 1.00 | VG | C | J1424-6807 | 2.70 | 0.85 | VG | N |
| J0253-5441 | 0.85 | 1.00 | VG | C | J1427-4206 | 3.89 | 0.75 | G | C |
| J0311-7651 | 1.50 | 0.91 | VG | N | J1512-5640 | 12.96 | 0.16 | B | C |
| J0335-5430 | 1.27 | 1.00 | VG | C | J1515-5559 | 3.67 | 1.00 | VG | C |
| J0450-8101 | 1.66 | 0.90 | VG | C | J1624-6809 | 4.59 | 0.78 | G | C |
| J0529-7215 | 0.70 | 1.00 | VG | C | J1628-6152 | 1.62 | 1.00 | VG | C |
| J0743-6726 | 1.79 | 1.00 | VG | C | J1703-6212 | 2.35 | 0.92 | VG | C |
| J0904-5735 | 1.10 | 0.96 | VG | N | J1744-5144 | 9.30 | 0.43 | B | C |
| J1038-5311 | 4.19 | 0.69 | G | C | J1803-6507 | 0.98 | 1.09 | VG | C |
| J1041-4740 | 1.88 | 1.00 | VG | C | J1809-4552 | 2.32 | 1.00 | VG | C |
| J1051-5344 | 5.22 | 0.76 | G | C | J1837-7108 | 1.49 | 1.00 | VG | C |
| J1101-6325 | 3.89 | 0.50 | G | C | J1912-8010 | 1.30 | 1.00 | VG | C |
| J1107-6820 | 1.72 | 1.00 | VG | N | J1930-6056 | 6.06 | 0.88 | G | C |
| J1112-5703 | 5.91 | 0.34 | I | N | J1940-6907 | 1.54 | 1.00 | VG | C |
| J1131-5818 | 1.78 | 0.93 | VG | C | J2035-6846 | 0.76 | 1.00 | VG | C |
| J1145-6954 | 1.15 | 0.85 | VG | C | J2105-7825 | 1.59 | 1.00 | VG | C |
| J1151-6728 | 5.08 | 0.86 | G | C | J2147-7536 | 1.06 | 1.00 | VG | C |
| J1206-6138 | 15.07 | 0.30 | B | C | J2152-7807 | 1.10 | 1.00 | VG | N |
| J1252-6737 | 1.84 | 1.00 | VG | C | J2303-6807 | 0.61 | 1.00 | VG | C |
| J1254-7138 | 1.36 | 0.89 | VG | C | J2336-5236 | 1.27 | 1.00 | VG | N |
| J1315-5334 | 3.44 | 0.80 | VG | C | J2356-6820 | 1.55 | 1.00 | VG | C |
| J1355-6326 | 19.30 | 0.13 | B | N | | | | | |

[3] A source listed as calibrator in the RFC is a source which has 8 or more detections at both 2.3 and 8.4 GHz, and has position accuracy better than 25 nrad.

[4] A source listed as non-calibrator in the RFC is a source which has at least 8 detections at either 2.3 or 8.4 GHz, and has position accuracy in the range [25, 500] nrad.

## 5. Summary and Conclusion

Our first interest in this research was to determine the suitability of our sources as calibrators for 1.4-GHz band observations. The two important properties we need from good calibrator sources are that they should be very bright and compact. Calibrator sources should also have accurately known positions. Among the 43 sources, we found that 38 sources are in the good or very good calibrator classes. Of the 38 sources 32 sources have accurately determined source positions in the RFC. Therefore, these 32 sources are good calibrators for global-array VLBI observations at 1.6 GHz.

After determining the suitability of the sources as calibrators, our second interest was to figure out how safe it is to use known 8.4 GHz calibrators for 1.4-GHz band observations. We found that 91% of the sources known to be good calibrators at 8.4 GHz are still good for 1.4-GHz band observations. This result is mainly important as the number of known calibrator sources in the 1.4-GHz band is very small, while there are many more known calibrator sources at 8.4 GHz observations from which we could get usable calibrator sources for 1.4-GHz band observations with 91% chance.

## Acknowledgments

This research was supported by the National Space Science Program (NASSP), Hartebeesthoek radio Astronomy Observatory (HartRAO) and the National Research Foundation (NRF).

## References

[1] Beasley A J. Gordon D, Peck A B, Petrov L, MacMillan D S, Fomalont E B and Ma C 2002 *ApJS* **141** 13-21
[2] Booth, R. S. and Jonas J. L 2012 *African Skies* **16** 101-04
[3] Briggs D S, Schwab F R and Sramek R A 1999 *ASPC* **180** 127-149
[4] Cornwell T, Braun R, Briggs D S 2004 *Synthesis Imaging in Radio Astronomy II, ASP Conference Series* **180** 151-70
[5] Clark B G 1995 *ASPC* **82** 3-16
[6] Fomalont E B, Petrov L, MacMillan D S, Gordon D and Ma C 2003 *AJ* **126** 2562-66
[7] Gaylard M J,et al. 2011 *SAIP* 473-78
[8] Hungwe F, Ojha R, Booth R S, Bietenholz M F, Collioud A, Charlot P, Boboltz D and Fey A L 2011 *MNRAS* **418** 2113-20
[9] Johnston S, et al. 2008 *Experimental Astronomy* **22** 151-273
[10] Kovalev Y Y, Petrov L, Fomalont E B and Gordon D 2007 *AJ* **133** 1236-43
[11] Ojha R, et al. 2004 *AJ* **127** 3609-21
[12] Petrov L, Phillips C, Bertarini A, Murphy T and Sadler E M 2011 *MNRAS* **414** 2528-39
[13] Petrov L, Kovalev Y Y, Fomalont E B and Gordon D 2005 *AJ* **129** 1163-70
[14] Petrov L, Kovalev Y Y, Fomalont E B and Gordon D 2006 *AJ* **131** 1872-79
[15] Petrov L, Kovalev Y Y, Fomalont E B and Gordon D 2008 *AJ* **136** 580-85